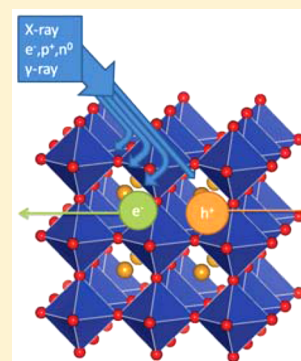


Methylammonium Lead Iodide for Efficient X-ray Energy Conversion

Bálint Náfrádi,^{*,†} Gábor Náfrádi,[‡] László Forró,[†] and Endre Horváth[†][†]Laboratory of Physics of Complex Matter, Ecole Polytechnique Fédérale de Lausanne (EPFL), CH-1015 Lausanne, Switzerland[‡]Institute of Nuclear Techniques (NTI), Budapest University of Technology and Economics (BME), H-1111 Budapest, Hungary

ABSTRACT: We report on photocurrent generation by X-ray irradiation in methylammonium lead iodide $\text{CH}_3\text{NH}_3\text{PbI}_3$ single crystals. We observed 75% of charge collection efficiency in millimeter sized samples. This efficiency is partially due to the high photon absorption coefficient and X-ray beam stopping power of our lead containing material. The material shows a less than 20% decrease in its performance up to 40 Sv of total X-ray dose, which represents a very good stability. Moreover, our Monte Carlo N-Particle Transport calculations indicate that energetic particle radiation can also be harvested by $\text{CH}_3\text{NH}_3\text{PbI}_3$. These properties are compared to $\text{CH}_3\text{NH}_3\text{SnI}_3$ and PbI_2 . The possible application of these advantageous properties could be in simultaneous radiation protection and direct electricity production in environments with highly energetic background radiation.



INTRODUCTION

Photon harvesting for direct electricity conversion is an important method for renewable energy production. In traditional photovoltaics, only the visible spectral range of solar radiation is converted into direct current electricity. To increase the conversion efficiency, efforts are made to extend the spectral range of photovoltaic devices toward infrared energies because it contains about one-half of the total radiated energy of the sun. The real breakthrough would be a fabrication of photovoltaic cells where additionally UV or even higher energy photons are harvested and converted into electricity.¹ However, the further increase of photon energies toward X-rays and γ -rays would amplify the radiation damage of conventional solar cells.^{2,3} This is a major challenge in photovoltaic energy conversion in outer space. Conventional solar cells must be protected from the high energy part of the solar spectrum.⁴ Producing solar panels that can withstand high radiation doses without efficiency loss is a prerequisite for economical astronautic applications. This idea already came up in the late 1960s to overcome the difficulties of photovoltaic energy conversion on the Earth's surface linked to atmospheric absorption, daily downtime, dusting, or shading, but the project was on stand-by until recently.^{5,6} However, there is a renowned interest for outer space-based solar power collection. For example, the Japan Aerospace Exploration Agency published a technology roadmap, which proposes the development of a 1 GW solar energy-based power plant by the 2030s.⁷ Recently, a promising trial was demonstrated to overcome the UV sensitivity of solar cells.⁸ Additionally, structures that not only endure high radiation dose but also convert it into electricity would be very beneficial. This would also have far reaching consequences in converting waste X- and even γ -ray radiation in nuclear power plants.

$\text{CH}_3\text{NH}_3\text{PbI}_3$ -based solar cells are promising candidates for space-based solar energy production. On the one hand, cells

based on this material ensure visible light efficiencies above 20%, which is a remarkable achievement.⁹ The Shockley–Queisser limit for the efficiency of single-junction $\text{CH}_3\text{NH}_3\text{PbI}_3$ solar cells is in reach.¹⁰ On the other hand, the precursor compound PbI_2 , whose building units are present in $\text{CH}_3\text{NH}_3\text{PbI}_3$, is a known X- and γ -ray detector.^{11,12} Indeed, very recently, $\text{CH}_3\text{NH}_3\text{PbI}_3$ demonstrated energy-harvesting through the gammavoltaic effect and was proposed as a potent X-ray detector material.^{13,14} This was demonstrated experimentally subsequently.¹⁵ The combination of these facts suggests the possibility of fabricating solar cells for harvesting both visible and also X-ray and γ -ray photons.

Here, we report the possibility of fabricating high-efficiency photovoltaic cells for X-ray harvesting based on methylammonium lead iodide, $\text{CH}_3\text{NH}_3\text{PbI}_3$. We found a high-efficiency current conversion for X-ray radiation, which goes together with a high X-ray absorption coefficient. Moreover, the material shows a long-term stability for high radiation doses. Our calculations indicate that energetic particle radiation can also be harvested by $\text{CH}_3\text{NH}_3\text{PbI}_3$. On the basis of these results, we propose the possible application of this material for energy conversion in radiation-rich environments such as outer space, nuclear power plants, etc. The radiation shielding properties of $\text{CH}_3\text{NH}_3\text{PbI}_3$ are compared to those of $\text{CH}_3\text{NH}_3\text{SnI}_3$ and PbI_2 .

EXPERIMENTAL METHODS

$\text{CH}_3\text{NH}_3\text{PbI}_3$ single crystals were prepared by precipitation from a concentrated aqueous solution of hydriodic acid (57 wt % in H_2O , 99.99% Sigma-Aldrich) containing lead(II) acetate trihydrate (99.999%, Acros Organics) and a respective amount

Received: August 13, 2015

Revised: October 16, 2015

Published: October 16, 2015

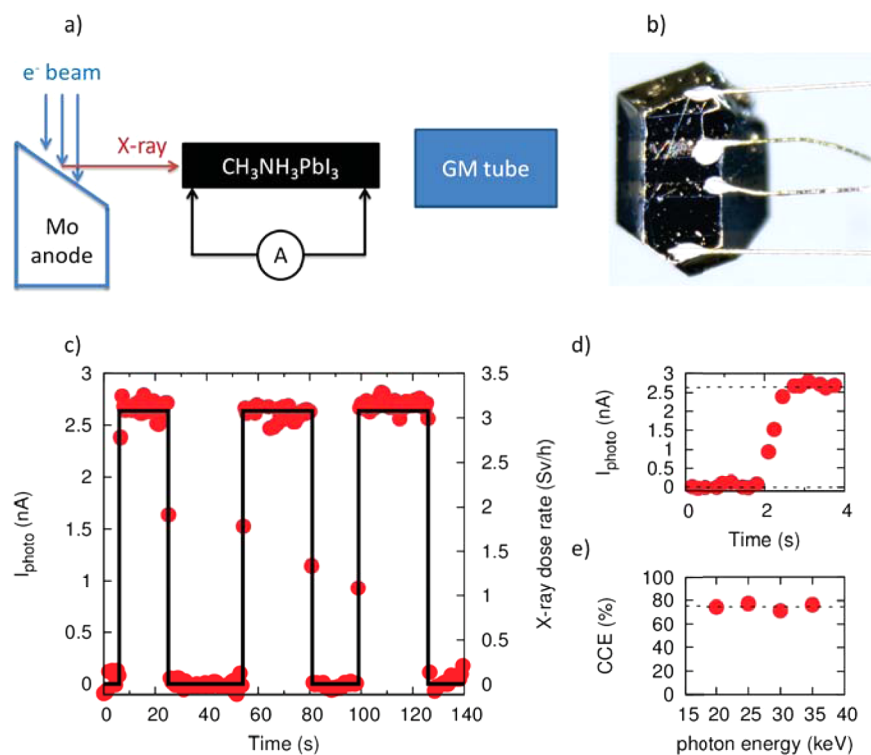


Figure 1. (a) Schematic drawing of the experimental setup. (b) Photograph of a typical $\text{CH}_3\text{NH}_3\text{PbI}_3$ single crystal with gold wires for photocurrent measurements. (c) X-ray illumination-induced photocurrent as a function of time (points) for $\text{CH}_3\text{NH}_3\text{PbI}_3$. The continuous line is showing the time variation of the X-ray flux. (d) The on–off response time of $\text{CH}_3\text{NH}_3\text{PbI}_3$ is shorter than 1 s, which is the instrumental time resolution of our setup. The on- and off-dynamics is symmetric, which contrasts with the asymmetry in on–off-speed and minute-long slow dynamics reported for visible light illumination. (e) Charge collection efficiency, CCE, as a function of photon energy is about 75%.

of CH_3NH_2 solution (40 wt % in H_2O , Sigma-Aldrich). A constant 55–42 °C temperature gradient was applied to induce the saturation of the solute at the low temperature part of the solution. Large $\text{CH}_3\text{NH}_3\text{PbI}_3$ crystals with 20–25 mm length and 10 mm diameter were grown after 7 days. Leaving the crystals in open air resulted in a silver-gray to green-yellow color change. To prevent this unwanted reaction with moisture, the as-synthesized crystals were immediately transferred and kept in a desiccator prior to the measurements. For the experiments, a single crystal with $m = 10(1)$ mg mass was selected.

X-ray absorption and photocurrent generation was measured in a Leybold X-ray apparatus. A 42 kW Mo X-ray tube was operated with $U = 20\text{--}35$ kV acceleration voltage and $I = 0\text{--}1$ mA current range. For X-ray detection, a calibrated Geiger–Müller tube (G–M tube) was used. Figure 1 a depicts the experimental setup.

The X-ray generated photocurrent was measured by a Keithley 2400 General-Purpose SourceMeter in a two-terminal geometry under fixed DC-bias in a 0–1 V/mm range. The photocurrent experiments were performed in ambient atmosphere with 30% relative humidity at 23 °C. The reported X-ray induced photocurrent, I_{photo} , is the difference of the current measured by X-rays on and off. Thus, it is unaffected by visible light radiation effects.

The X-ray mass attenuation coefficient μ_m of $\text{CH}_3\text{NH}_3\text{PbI}_3$ was measured by a calibrated G–M tube placed after a pinhole. The pinhole was empty or completely covered by a 0.4 mm thick single crystal of $\text{CH}_3\text{NH}_3\text{PbI}_3$.

The calculated value of the mass attenuation coefficient, μ_m , for $\text{CH}_3\text{NH}_3\text{PbI}_3$ was determined by the equation:

$$\mu_m = \sum_i w_i (\mu_m)_i \quad (1)$$

where w_i is the weight fraction of the i th atomic constituent as the tabulated values for each constituting element by Seltzer.¹⁶

The charge collection efficiency, CCE, was calculated as the ratio of the number of X-ray photon-induced electrons estimated from eq 2 and the number of collected electrons $N_e^- = I_{\text{photo}}/q$, where q is the elementary charge.

The theoretical Monte Carlo calculations were carried out by the Monte Carlo N-Particle Transport code (MCNP6 version 1.0).¹⁷ These calculations require one to define a geometrical model, which was designed by SuperMc/MCAM 5.2.¹⁸ The model contained four regions. The source region was a 100 cm \times 100 cm plane, where the initial beam (photons, electrons, or neutrons) was homogeneously sampled and launched toward to the target cell. The momentum of these particles was perpendicular to the front surface of the target cell. The distance between the source and the target was 1 m, and it was filled by vacuum. The front surface of the target cell was 100 cm \times 100 cm. The volume of the target cell was homogeneously filled by $\text{CH}_3\text{NH}_3\text{PbI}_3$, $\text{CH}_3\text{NH}_3\text{SnI}_3$, or PbI_2 . After the target cell, a second vacuum cell was defined with 1 m length. For the neutron calculations, the ENDF70a cross section library was used. The treatment of the electrons and other charged particles uses the el103 library. Doses were calculated by the F6 tally, while the volume averaged spectra were calculated by the F4 tally. All results were normalized to one launched particle and to the 0.02 MeV energy bin.

RESULTS AND DISCUSSION

There are several material requirements for high-efficiency photovoltaic applications and high-energy radiation harvesting. The material should have high beam stopping power and convert the absorbed energy to electron–hole pairs. Moreover, the photogenerated charges should be efficiently extracted from the material. At photon energies, much higher than the band gap (Δ) of the semiconducting material, the photoeffect, that is, direct photon to electron–hole pair conversion, is independent of the structural details of the material. The number of electron–hole pairs, N_{pairs} , is directly proportional to the absorbed dose, D , and inversely proportional to the electron–hole pair creation energy, expressed by the empirical relation $E_{e-h} = 2\Delta + 1.43 \text{ eV}$.¹⁹ In a unit mass of matter, it gives

$$N_{\text{pairs}} = \frac{D}{E_{e-h}} \quad (2)$$

Consequently, a prerequisite for high efficiency radiation to electricity conversion is a high mass attenuation coefficient, μ_m . A material with a high μ_m will attenuate the radiation quickly, and thus most of the energy is absorbed in the crystal. Here, we determined the mass attenuation coefficient of $\text{CH}_3\text{NH}_3\text{PbI}_3$ for soft X-ray radiation by the exponential attenuation law:²⁰

$$\mu_m = \frac{1}{x} \ln \frac{I_0}{I_x} \quad (3)$$

where $x = 0.4 \text{ mm}$ is the thickness of our $\text{CH}_3\text{NH}_3\text{PbI}_3$ crystal. The initial beam intensity $I_0 = 530 \pm 23 \text{ counts s}^{-1}$ dropped to $I_x = 50 \pm 7 \text{ counts s}^{-1}$ while passing through our $\text{CH}_3\text{NH}_3\text{PbI}_3$. This yields $\mu_m = 14 \pm 1.2 \text{ cm}^2 \text{ g}^{-1}$. This is in rather good agreement with calculations based on the additivity of elemental $\mu_m^{\text{calc}} = 15.4 \text{ cm}^2 \text{ g}^{-1}$ for a 30 keV X-ray photon energy (eq 1).^{16,20} It clearly outperforms Si ($1.436 \text{ cm}^2 \text{ g}^{-1}$), and it is comparable to PbI_2 ($18.34 \text{ cm}^2 \text{ g}^{-1}$).¹⁶ For instance, the half-value layer, the thickness of the material at which the intensity of radiation entering it is reduced by one-half, is only $110 \mu\text{m}$ at soft X-ray energies for $\text{CH}_3\text{NH}_3\text{PbI}_3$, while it is almost 1 mm for Si.

The high absorption coefficient is a required but not sufficient criterion for X-ray photovoltaic applications. The photo excited charges have to be efficiently extracted from the bulk of the material as well; that is, the charge collection efficiency (CCE) must be also high. To determine the CCE of $\text{CH}_3\text{NH}_3\text{PbI}_3$ for 20–35 keV soft X-ray irradiation, we measured the photocurrent with fixed potential difference across a $\text{CH}_3\text{NH}_3\text{PbI}_3$ single crystal. The key finding of our work is the very high CCE of $75 \pm 6\%$ of $\text{CH}_3\text{NH}_3\text{PbI}_3$ for 20–35 keV soft X-ray irradiation (Figure 1). This means that about 75% of the X-ray generated photo electrons estimated by eq 2 were collected in the form of electric current. This is even more remarkable in view that the distance between the source/drain contacts is 2.5 mm in our experiments; thus photoexcited carriers propagated over extended distances. This finding is in agreement with recent single crystal studies where electron diffusion lengths exceeding $\sim 200 \mu\text{m}$ were found.^{13,21}

The visible light-induced photoresponse of $\text{CH}_3\text{NH}_3\text{PbI}_3$ shows strong hysteresis and asymmetry in on–off cycles and slow time dynamics.^{22–24} This is attributed to surface defects and trap states of $\text{CH}_3\text{NH}_3\text{PbI}_3$. In X-ray-induced photoresponse, however, radiation is absorbed in the bulk of the material; thus surface related trap-states are expected to play a secondary role only. To better characterize the X-ray

photocurrent generation, the time-response to the X-ray illumination was studied, shown in Figure 1. Both the rise- and the fall-times of the X-ray photocurrent are below 1 s , the instrumental time resolution of our experiment. The fast time characteristic, and the symmetric on–off time for X-ray illumination, is in contrast to the asymmetric, slow, minute time-scale dynamics reported for $\text{CH}_3\text{NH}_3\text{PbI}_3$ under visible light illumination.^{23,25,26} These findings indicate that the slow relaxation and asymmetry are mainly a surface related phenomenon linked to the sub-micrometer penetration depth of visible light. This is not the case for X-rays, which penetrate to the bulk of the material.

The reported values for quantum efficiency of $\text{CH}_3\text{NH}_3\text{PbI}_3$ for visible light vary a lot depending on the morphology, crystallinity of the sample, the light intensity, and its wavelength. To characterize the about 75% charge collection efficiency observed for the high 3000 mSv/h dose rate for soft X-ray, we performed a systematic study as a function of X-ray dose. We found that above $\sim 500 \text{ mSv/h}$, I_{photo} increases linearly with 3 Sv/h dose rate up to the highest exposed quantities (Figure 2). A linear fit of the high dose rate

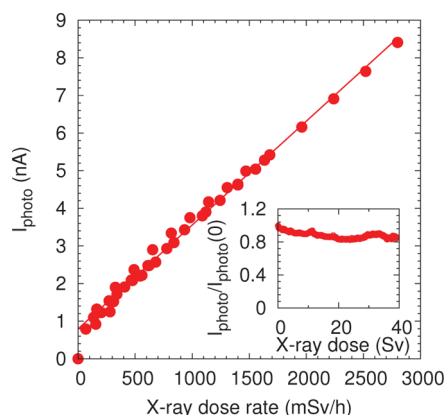


Figure 2. Photocurrent as a function of X-ray dose rate for a $\text{CH}_3\text{NH}_3\text{PbI}_3$ single crystal. The inset shows the stability of the photocurrent as a function of X-ray dose. The 40 Sv value is 2 orders of magnitude higher than the yearly exposure of the International Space Station.

measurements extrapolates to finite zero dose value. This indicates that at the smallest dose rates, I_{photo} increases much faster than above $\sim 500 \text{ mSv/h}$. This observation is in good agreement with low light-power studies in a visible spectral range where extremely large photosensitivity was observed, indicating a feasibility of even single photon detection.²⁶

A crucial parameter for applications is the long-term stability of the photovoltaic material against radiation damage. We followed I_{photo} as a function of the deployed X-ray dose up to a total dose of 40 Sv (Figure 2, inset). Remarkably, the photocurrent dropped by less than 20% by 40 Sv dose (2 days of continuous irradiation). Note that an average yearly dose received by the International Space Station is less than 200 mSv .²⁷ Moreover, the $\text{CH}_3\text{NH}_3\text{PbI}_3$ sample was not protected from air humidity during the 2 days of irradiation. It is very likely that part of the performance degradation could occur due to chemical degradation of the sample instead of radiation damage; that is, the $\sim 20\%$ efficiency drop could be at least partially due to humidity effects.^{28,29} This demonstrates the high stability of $\text{CH}_3\text{NH}_3\text{PbI}_3$ against X-ray radiation.

If one thinks of outer space applications where ionizing radiation is present, one has to note that it consists not only of photons but also of other highly energetic particles. In astronautics, the particle radiation is predominantly composed of electrons and protons from the solar wind. It is transformed to photon radiation during the interaction with solids via bremsstrahlung. The bremsstrahlung in principle could be harvested in the form of electricity when the photovoltaic material possesses high mass attenuation coefficient and can sustain high radiation dose without significant performance loss. The aforementioned characteristics of the $\text{CH}_3\text{NH}_3\text{PbI}_3$ system offer precisely this novel functionality. We propose that $\text{CH}_3\text{NH}_3\text{PbI}_3$ could be used to convert a particle beam to photons by bremsstrahlung, which would then internally converted into electricity. Indeed, electron radiation in the in situ scanning electron microscope measurements showed photocurrent generation by e^- -beam exposure without reported sample degradation.³⁰ The e^- -beam induced luminescence experiments showed no sample degradation either.²⁵ The remarkable stability of $\text{CH}_3\text{NH}_3\text{PbI}_3$ against radiation damage is proposed to be a consequence of the ionic bonding present in the material.³¹ These results indicate the feasibility of the proposed particle radiation to electricity conversion.

Here, we quantify the first step, the photon generation, by Monte Carlo calculations. We do so in view of the possible application of converting the impact of highly energetic particles into photons and then to photoelectrons, which could serve in photovoltaics. Figure 3 shows the calculated

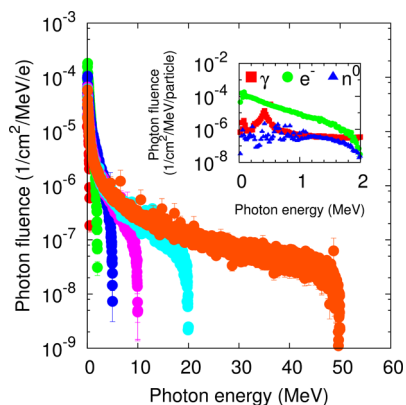


Figure 3. Calculated photon spectrum generated by e^- irradiation passing through 1 mm $\text{CH}_3\text{NH}_3\text{PbI}_3$. Spectra from left to right correspond to 0.5, 2, 5, 10, 20, and 50 MeV e^- energy, respectively. The inset shows the calculated photon spectrum for 2 MeV energy photon, electron, and neutron irradiation.

photon spectra inside the bulk of $\text{CH}_3\text{NH}_3\text{PbI}_3$ resulting from bombardment by energetic electrons between 0.5 and 50 MeV. A common feature for bremsstrahlung is a continuous photon spectrum produced with cutoff energy equal to the incoming particle energy. The inset of Figure 3 shows the calculated photon spectrum generated by bombardment of various 2 MeV energy particles (γ , e^- , n^0). This photon radiation generated by incoming particle radiation can be immediately harvested by $\text{CH}_3\text{NH}_3\text{PbI}_3$ due to its high quantum efficiency in the X-ray and γ -ray regions.^{13,15} Moreover, the calculations also show that the electron transmission for the 1 mm thick $\text{CH}_3\text{NH}_3\text{PbI}_3$ plate is only 3.15×10^{-5} for an electron energy of 2 MeV. Thus, $\text{CH}_3\text{NH}_3\text{PbI}_3$ is a good radiation shielding material, which renders a multifunctional character to the material where

the high beam stopping power and electricity harvesting possibilities are merged.

Monte Carlo calculations were also performed for $\text{CH}_3\text{NH}_3\text{SnI}_3$ and PbI_2 . The photon absorption properties of 1 mm thick $\text{CH}_3\text{NH}_3\text{PbI}_3$, $\text{CH}_3\text{NH}_3\text{SnI}_3$, and PbI_2 plates are compared in Figure 4. Radiation below 0.1 MeV energy is

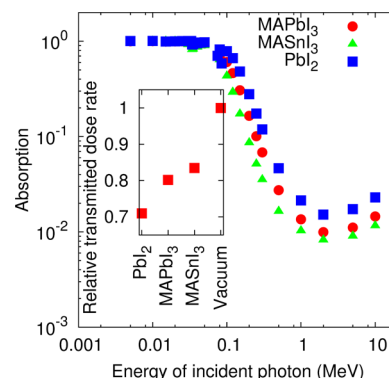


Figure 4. Calculated energy absorption of 1 mm thick plates as a function of photon energy for different materials as indicated by the caption. MA stands for CH_3NH_3 . The inset shows the transmitted dose rate of 2 MeV incoming photons relative to a vacuum.

completely absorbed by a 1 mm thick material. At higher energies, however, they become semitransparent as expected from eq 3. The shielding properties are characterized at photon energies of 2 MeV for 20 mm thick plates (Figure 4 inset). $\text{CH}_3\text{NH}_3\text{PbI}_3$ slightly outperforms $\text{CH}_3\text{NH}_3\text{SnI}_3$, but both compounds are comparable to PbI_2 .

In addition to space-based solar energy conversion, one could think of harvesting waste radiation in nuclear energy production lines like fission and fusion power plants, as well. In fission power plants, a large amount of heavy concrete is used for biological shielding to reduce the effective dose of particles, γ -rays, and X-rays. A layer of $\text{CH}_3\text{NH}_3\text{PbI}_3$ could maintain biological shielding, but at the same time electricity could be produced. Also, in future fusion power plants, the high photon radiation dose on the vessel could be directly turned into electricity. For instance, in ITER a $10\text{--}30$ keV photon flux is expected to exceed $10^{13}/\text{keV}/\text{s}/\text{cm}^3$ at the walls of the plasma vessel.³² Over the entire surface of ITER, this means about 50 kW waste energy.³² This waste radiation could be harvested by a $\text{CH}_3\text{NH}_3\text{PbI}_3$ biological shielding layer.

CONCLUSIONS

We reported a high $\mu_m = 14 \pm 1.2$ $\text{cm}^2 \text{g}^{-1}$ value and $75 \pm 6\%$ charge collection efficiency for unfiltered X-ray radiation in the 20–35 keV range and a high photon absorption coefficient for $\text{CH}_3\text{NH}_3\text{PbI}_3$ bulk crystals. It was also found that this material has a high stability against X-ray radiation over an extended dose range. They allow novel functionalities of energy production and shielding in environments with high background radiation such as in outer space, and in fission- and fusion-power plants.

AUTHOR INFORMATION

Corresponding Author

*Phone: +41 21 69 34515. Fax: +41 21 693 4470. E-mail: balint.nafraadi@epfl.ch.

Notes

The authors declare no competing financial interest.

ACKNOWLEDGMENTS

The technical help of Andrea Pisoni (EPFL) with the photocurrent experiments is gratefully acknowledged. The work in Lausanne was supported by the Swiss National Science Foundation (Grant No. 200021_144419) and ERC advanced grant "PICOPROP" (Grant No. 670918).

REFERENCES

- (1) Wu, J.; Yue, G.; Xiao, Y.; Lin, J.; Huang, M.; Lan, Z.; Tang, Q.; Huang, Y.; Fan, L.; Yin, S.; et al. An Ultraviolet Responsive Hybrid Solar Cell Based on Titania/poly(3-hexylthiophene). *Sci. Rep.* **2013**, *3*, 1283.
- (2) Tada, H.; Carter, J. In *Solar Cell Radiation Handbook*; Anspaugh, B. E., Downing, R., Eds.; NASA, 1982.
- (3) Moll, M. Radiation Damage in Silicon Particle Detectors - Microscopic Defects and Macroscopic Properties. Ph.D. Thesis, Universitat Hamburg, 1999.
- (4) Meulenberg, A., Jr. *Ultraviolet Damage in Solar Cell Assemblies with Various UV Filters*; NASA. Lewis Res. Center Solar Cell High Efficiency and Radiation Damage (SEE N78-13527 04-44), 1977; pp 227–229.
- (5) Glaser, P. E. Power From the Sun: Its Future. *Science* **1968**, *162*, 857–861.
- (6) Roebuck, K. *Photovoltaics (PV): High-impact Strategies - What You Need to Know: Definitions, Adoptions, Impact, Benefits, Maturity, Vendors*; Dayboro: Emereo Publishing, 2012.
- (7) Little, F. E. Solar Power Satellites: Recent Developments. *XXVIIth General Assembly of the International Union of Radio Science*, 2002.
- (8) Leijtens, T.; Eperon, G. E.; Pathak, S.; Abate, A.; Lee, M. M.; Snaith, H. J. Overcoming Ultraviolet Light Instability of sensitized TiO₂ With Meso-superstructured Organometal Tri-halide Perovskite Solar Cells. *Nat. Commun.* **2013**, *4*, 2885.
- (9) Park, N.-G. Organometal Perovskite Light Absorbers Toward a 20% Efficiency Low-Cost Solid-State Mesoscopic Solar Cell. *J. Phys. Chem. Lett.* **2013**, *4*, 2423–2429.
- (10) Snaith, H. J. Perovskites: The Emergence of a New Era for Low-Cost, High-Efficiency Solar Cells. *J. Phys. Chem. Lett.* **2013**, *4*, 3623–3630.
- (11) Henisch, H.; Srinivasagopalan, C. Properties of Semiconducting Lead Iodide. *Solid State Commun.* **1966**, *4*, 415–418.
- (12) Lund, J.; Shah, K.; Squillante, M.; Moy, L.; Sinclair, F.; Entine, G. Properties of Lead Iodide Semiconductor Radiation Detectors. *Nucl. Instrum. Methods Phys. Res., Sect. A* **1989**, *283*, 299–302.
- (13) Dong, Q.; Fang, Y.; Shao, Y.; Mulligan, P.; Qiu, J.; Cao, L.; Huang, J. Electron-hole Diffusion Lengths > 175 μm in Solution-grown CH₃NH₃PbI₃ Single Crystals. *Science* **2015**, *347*, 967–970.
- (14) Horváth, E.; Forró, L.; Spina, M. *Nanowires of Organic-Inorganic Perovskites*. International Patent Application no. PCT/IB2014/061649, May 23, 2014.
- (15) Yakunin, S.; Sytnyk, M.; Krieger, D.; Shrestha, S.; Richter, M.; Matt, G. J.; Azimi, H.; Brabec, C. J.; Stangl, J.; Kovalenko, M. V.; et al. Detection of X-ray Photons by Solution-processed Lead Halide Perovskites. *Nat. Photonics* **2015**, *9*, 444–449.
- (16) Seltzer, S. M. Calculation of Photon Mass Energy-Transfer and Mass Energy-Absorption Coefficients. *Radiat. Res.* **1993**, *136*, 147–170.
- (17) Goorley, T.; James, M.; Booth, T.; Brown, F.; Bull, J.; Cox, J.; Durkee, J.; Elson, J.; Fensin, M.; Forster, R. A.; et al. Initial MCNP6 Release Overview. *Nucl. Technol.* **2012**, *180*, 298–315. LA-UR-13-22934.
- (18) Wu, Y. FDS Team, CAD-based Interface Programs for Fusion Neutron Transport Simulation. *Fusion Eng. Des.* **2009**, *84*, 1987–1992. Proceeding of the 25th Symposium on Fusion Technology (SOFT-25).
- (19) Devanathan, R.; Corrales, L.; Gao, F.; Weber, W. Signal Variance in Gamma-ray Detectors A Review. *Nucl. Instrum. Methods Phys. Res., Sect. A* **2006**, *565*, 637–649.
- (20) Gerward, L. X-ray Attenuation Coefficients: Current State of Knowledge and Availability. *Radiat. Phys. Chem.* **1993**, *41*, 783–789.
- (21) Shi, D.; Adinolfi, V.; Comin, R.; Yuan, M.; Alarousu, E.; Buin, A.; Chen, Y.; Hoogland, S.; Rothenberger, A.; Katsiev, K.; et al. Low trap-state Density and Long Carrier Diffusion in Organolead Trihalide Perovskite Single Crystals. *Science* **2015**, *347*, 519–522.
- (22) Kim, H.-S.; Park, N.-G. Parameters Affecting I V Hysteresis of CH₃NH₃PbI₃ Perovskite Solar Cells: Effects of Perovskite Crystal Size and Mesoporous TiO₂ Layer. *J. Phys. Chem. Lett.* **2014**, *5*, 2927–2934.
- (23) Gottesman, R.; Haltzi, E.; Gouda, L.; Tirosh, S.; Bouhadana, Y.; Zaban, A.; Mosconi, E.; De Angelis, F. Extremely Slow Photoconductivity Response of CH₃NH₃PbI₃ Perovskites Suggesting Structural Changes under Working Conditions. *J. Phys. Chem. Lett.* **2014**, *5*, 2662–2669.
- (24) Tress, W.; Marinova, N.; Moehl, T.; Zakeeruddin, S. M.; Nazeeruddin, M. K.; Grätzel, M. Understanding the Rate-dependent JV Hysteresis, Slow Time Component, and Aging in CH₃NH₃PbI₃ Perovskite Solar Cells: the Role of a Compensated Electric Field. *Energy Environ. Sci.* **2015**, *8*, 995–1004.
- (25) Horváth, E.; Spina, M.; Szekrényes, Z.; Kamarás, K.; Gaál, R.; Gachet, D.; Forró, L. Nanowires of Methylammonium Lead Iodide (CH₃NH₃PbI₃) Prepared by Low Temperature Solution-Mediated Crystallization. *Nano Lett.* **2014**, *14*, 6761–6766.
- (26) Spina, M.; Lehmann, M.; Náfrádi, B.; Bernard, L.; Bonvin, E.; Gaál, R.; Magrez, A.; Forr, L.; Horváth, E. Microengineered CH₃NH₃PbI₃ Nanowire/Graphene Phototransistor for Low-Intensity Light Detection at Room Temperature. *Small* **2015**, *11*, 4824–4828.
- (27) Kodaira, S.; Kawashima, H.; Kitamura, H.; Kurano, M.; Uchihori, Y.; Yasuda, N.; Ogura, K.; Kobayashi, I.; Suzuki, A.; Koguchi, Y.; et al. Analysis of Radiation Dose Variations Measured by Passive Dosimeters Onboard the International Space Station During the Solar Quiet Period (20072008). *Radiat. Meas.* **2013**, *49*, 95–102.
- (28) Yang, J.; Siempelkamp, B. D.; Liu, D.; Kelly, T. L. Investigation of CH₃NH₃PbI₃ Degradation Rates and Mechanisms in Controlled Humidity Environments Using in Situ Techniques. *ACS Nano* **2015**, *9*, 1955–1963.
- (29) Matsumoto, F.; Vorpahl, S. M.; Banks, J. Q.; Sengupta, E.; Ginger, D. S. Photodecomposition and Morphology Evolution of Organometal Halide Perovskite Solar Cells. *J. Phys. Chem. C* **2015**, *119*, 20810–20816.
- (30) Edri, E.; Kirmayer, S.; Henning, A.; Mukhopadhyay, S.; Gartsman, K.; Rosenwaks, Y.; Hodes, G.; Cahen, D. Why Lead Methylammonium Tri-Iodide Perovskite-Based Solar Cells Require a Mesoporous Electron Transporting Scaffold (but Not Necessarily a Hole Conductor). *Nano Lett.* **2014**, *14*, 1000–1004.
- (31) Trachenko, K.; Pruneda, M.; Artacho, E.; Dove, M. T. Radiation Damage Effects in the Perovskite CaTiO₃ and Resistance of Materials to Amorphization. *Phys. Rev. B: Condens. Matter Mater. Phys.* **2004**, *70*, 134112.
- (32) Seguin, F. H.; Petrasso, R. D.; Li, C. K. Radiation-hardened X-ray Imaging for Burning-plasma Tokamaks. *Rev. Sci. Instrum.* **1997**, *68*, 753–756.